



**Calhoun: The NPS Institutional Archive**  
**DSpace Repository**

---

Faculty and Researchers

Faculty and Researchers' Publications

---

2017

# Effects of Mean Speed on Broadside SAR Imagery Signatures for Accelerating Targets

Garren, David A.

---

Garren, David A. "Effects of mean speed on broadside SAR imagery signatures for accelerating targets.", International Conference on Radar Systems (Radar 2017) pp.1-6. (2017).

<http://hdl.handle.net/10945/59008>

---

This publication is a work of the U.S. Government as defined in Title 17, United States Code, Section 101. Copyright protection is not available for this work in the United States.

*Downloaded from NPS Archive: Calhoun*



Calhoun is the Naval Postgraduate School's public access digital repository for research materials and institutional publications created by the NPS community. Calhoun is named for Professor of Mathematics Guy K. Calhoun, NPS's first appointed -- and published -- scholarly author.

**Dudley Knox Library / Naval Postgraduate School**  
**411 Dyer Road / 1 University Circle**  
**Monterey, California USA 93943**

<http://www.nps.edu/library>

# Effects of Mean Speed on Broadside SAR Imagery Signatures for Accelerating Targets

David A. Garren\*

\*Electrical and Computer Engineering Dept., Naval Postgraduate School, Monterey, California, USA, [dagarren@nps.edu](mailto:dagarren@nps.edu)

**Keywords:** Synthetic aperture radar, moving targets.

## Abstract

This paper examines the effects of the mean target speed on the synthetic aperture radar (SAR) imagery morphology of signatures induced by surface movers that are transitioning from a lower to higher speed during the collection interval. The radar platform moves with a constant velocity on a level flight path for the case of a broadside imaging geometry. Recent studies have revealed that such moving target smears are not constrained to have the simple shapes of mere parabolas but instead can display a rich variety of two-dimensional (2D) shapes, including self-crossing signatures. The current analysis investigates the properties of the theoretical 2D central contours of these smears under the conditions of varying the mean target speed for targets which transition from lower to higher speed. It is shown that these theoretical predictions of the signature contour morphology yield excellent agreement with the results of SAR image formation applied to simulated radar data.

## 1 Introduction

SAR data collections can yield high-fidelity imagery corresponding to a scene of interest on the earth's surface. However, any moving targets in the region are mismatched relative to the SAR image formation process and thus are often smeared in the radar cross-range direction within the resultant imagery. Many studies investigate the properties of signature smears in SAR imagery, which often arise from such moving targets within the scene. In particular, a number of researchers [1–4] investigate the general features of mover smears.

Some researchers [5–10] investigate moving target smear phenomenology using power series expansions of the motion-induced phase error, which tacitly supports the prior notion that moving target signatures always yield gently curved signatures having the shapes of approximate parabolas or hyperbolas. The use of power series expansions confounds the investigation of complicated target motions, since the number of terms in the resulting expansions becomes quite cumbersome [6, 11, 12]. The challenges of the power series expansion approach led to the development of subaperture-based techniques [13–18] for understanding moving target signatures. Subaperture-based

analyses have been performed by various researchers [19–22] investigating SAR concepts.

A number of researchers have analyzed the curved signature smears that result from moving targets in SAR imagery. In particular, Ref. [5] examines the signatures of constant velocity targets in stripmap SAR, which is related to range migration effects [23, 24]. For each subaperture within the collection, this study maximizes the target impulse response (IPR) integrated over a small but finite time interval of a scan SAR system. The resulting central contour of the signature smear corresponding to a constant velocity target is obtained by sliding this small time interval over the extent of the full aperture.

A recent analysis [13] also applies subaperture techniques in order to investigate spotlight SAR image signatures for surface targets moving with arbitrary motion for cases in which the radar trajectory has constant velocity on a straight and level flight path under conditions in which the radar mainbeam points in a direction which is broadside to that of the platform motion. This paper presents the first detailed study of SAR signature smears for cases of non-linear target motion. That is, the resulting equations give an analytic capability for predicting the 2D structure of moving target smears directly in terms of the ground-plane coordinates in which SAR imagery is generated. Refs. [17, 18] extend these results for cases of squinted collections. In addition, Reference [16] examines the special case of a target that transitions from a lower to higher speed during the SAR collection interval for broadside collection geometries. Such target motion can be modeled through the use of a hyperbolic tangent speed profile. The current analysis extends this work by examining the SAR signature morphology effects of varying the mean speed for targets which transition from lower to higher speeds.

## 2 General Target Signatures

Define a set of fixed three-dimensional (3D) Cartesian coordinates with the origin  $\{x, y, z\} = \{0, 0, 0\}$  lying at the surface location at which the radar steers its mainbeam during the full collection time. This coordinate origin is also referred to as the ground reference point (GRP). The coordinate  $z$  increases with altitude above the terrain, with  $z = 0$  defining the ground-plane. The coordinate  $x$  increases with ground down-range from the radar at the collection midpoint. The ground cross-range coordinate  $y$  completes the right-handed coordinates.

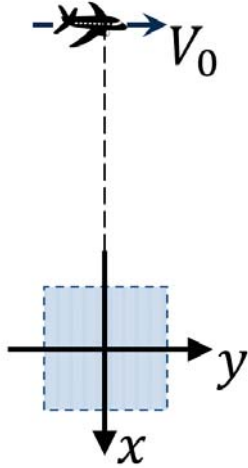


**Fig. 1:** This top view of the collection geometry shows the definitions of the ground plane coordinates  $x$  and  $y$  relative to the radar velocity vector.

The radar transmits a number of waveforms for a total collection duration of  $T_0$  between  $-T_0/2$  and  $T_0/2$ , so that  $t = 0$  is the synthetic aperture mid-point. During this collection interval, the target is permitted to move on the ground plane according to two arbitrary analytic functions of slow-time  $t$  in the ground down-range  $x$  and ground cross-range  $y$  directions:

$$x = \alpha(t), \quad y = \beta(t). \quad (1)$$

Define the following constant-velocity radar trajectory as a three-dimensional (3D) parameterization of position within the  $\{x, y, z\}$  coordinates as a function of slow-time  $t$ :

$$X(t) = -X_0, \quad (2)$$

$$Y(t) = \pm V_0 t, \quad (3)$$

$$Z(t) = Z_0. \quad (4)$$

Here,  $V_0$  is the constant radar speed. Also,  $X_0$  and  $Z_0$  are the values for the ground down-range and altitude, respectively, of the radar platform relative to the GRP at the aperture mid-time  $t = 0$ . The upper sign in (3) corresponds to a radar that pointed to the right, and the lower sign gives a radar pointing to the left. In the present convention, the upper sign gives a starboard-pointing radar mainbeam and the lower sign corresponds to one that is steered to the port side. This convention is used throughout this paper. In addition, define the following constant parameter:

$$\kappa_0 \equiv \mp \frac{X_0}{V_0}. \quad (5)$$

The  $n^{\text{th}}$  order derivatives of the true target motion functions  $\{\alpha(t), \beta(t)\}$  of (1) are applied to compute the corresponding  $\{x, y\}$  components of the instantaneous target position

$\{\mu_0(\tau_s), \nu_0(\tau_s)\}$  and velocity  $\{\mu_1(\tau_s), \nu_1(\tau_s)\}$  via:

$$\mu_n(\tau_s) = \left. \frac{d^n \alpha(t)}{dt^n} \right|_{t=\tau_s}, \quad \nu_n(\tau_s) = \left. \frac{d^n \beta(t)}{dt^n} \right|_{t=\tau_s}. \quad (6)$$

Here,  $\tau_s$  denotes the mean time for a given subaperture. Ref. [13] presents a methodology for computing the central contour of the SAR signature for a generic surface moving target. This locus corresponds to the location of energy deposition for a given subaperture image. This analysis yields the following generalized signature equations [13]:

$$x(\tau_s) = \mu_0(\tau_s) - \mu_1(\tau_s)\tau_s - \frac{1}{\kappa_0}\nu_1(\tau_s)\tau_s^2, \quad (7)$$

$$y(\tau_s) = \nu_0(\tau_s) + \kappa_0\mu_1(\tau_s) + \nu_1(\tau_s)\tau_s. \quad (8)$$

These equations give the size, shape, and location of the central contour of the signature smear induced by the moving target.

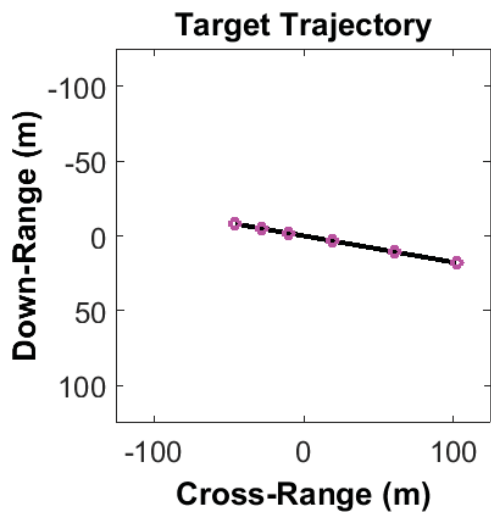
### 3 Signature Results

This section examines the specific signatures which result from individual cases of a constant-heading target which is initially moving with approximately constant speed and then undergoes an increase in speed, and then settles to a higher approximately constant speed with the same heading. All examples below examine the effects of different mean speeds for a given fixed target heading.

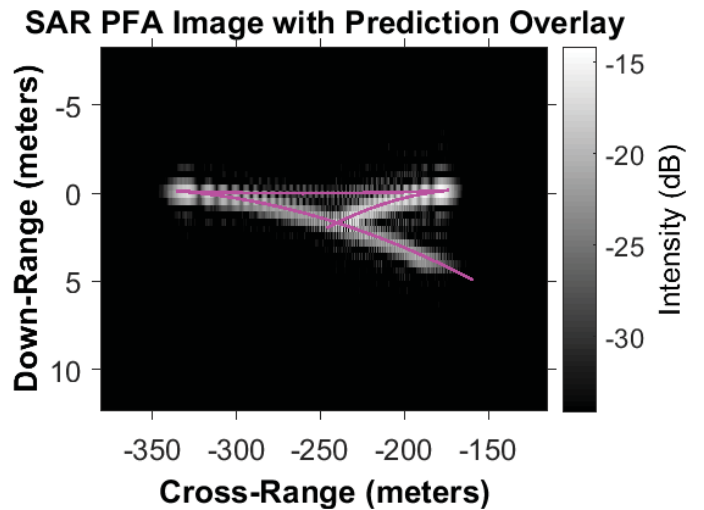
For the first example, the parameter values are selected to give the target trajectory of Figure 2(a) and the target speed of Figure 2(b). The induced SAR simulation signature smear and the prediction overlay for a rightward-pointing radar mainbeam are presented in Figure 3(a), and the corresponding results for a leftward-pointing radar are shown in Figure 3(b).

The signature shapes in these figures exhibit more structure than the simply bowed smear shapes that are characteristic of targets moving with constant speed and heading [13]. However, vehicle traffic in urban environments often undergoes frequent maneuvers in which the speed is increased, thus motivating the current research. In addition, this analysis of targets with increasing speed yields an accurate match between the predicted signatures and the actual target signature resulting from SAR simulations. Thus, these results further validate the predictive signature theory.

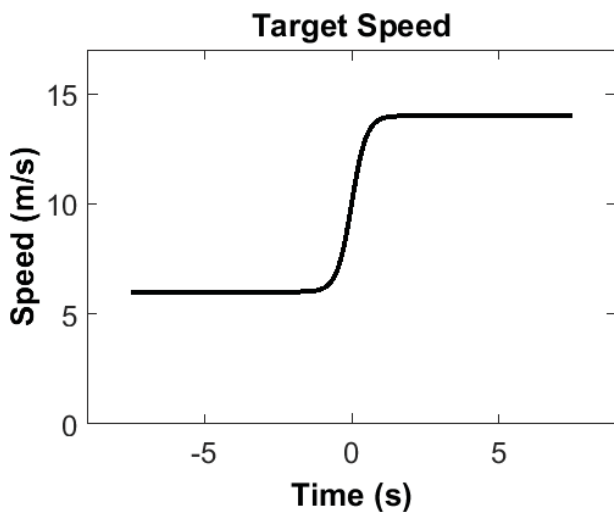
For the second set of examples, the mean speed is decreased relative to that of the first example. The true target trajectory and speed are shown in Figures 4(a) and 4(b), respectively. The induced signature smear and the corresponding prediction overlay are shown in Figure 5(a) for a rightward-pointing radar mainbeam and in Figure 5(b) for a leftward-pointing radar. Again, there is good agreement between the theoretical predictions and the results of the SAR simulation. The lower initial speed yields a smaller portion of the resulting signatures in these plots.



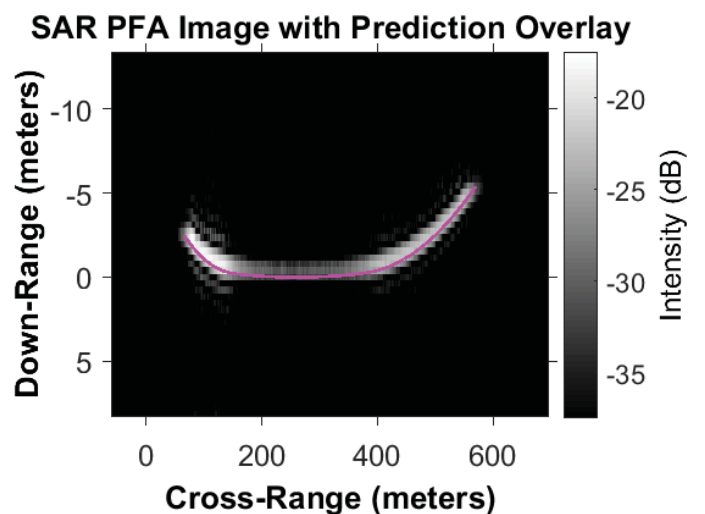
(a)



(a)



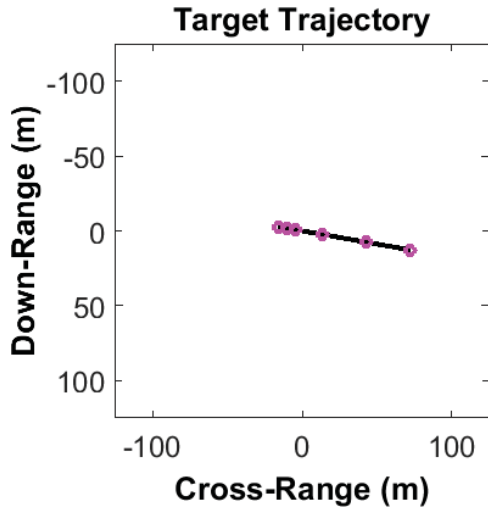
(b)



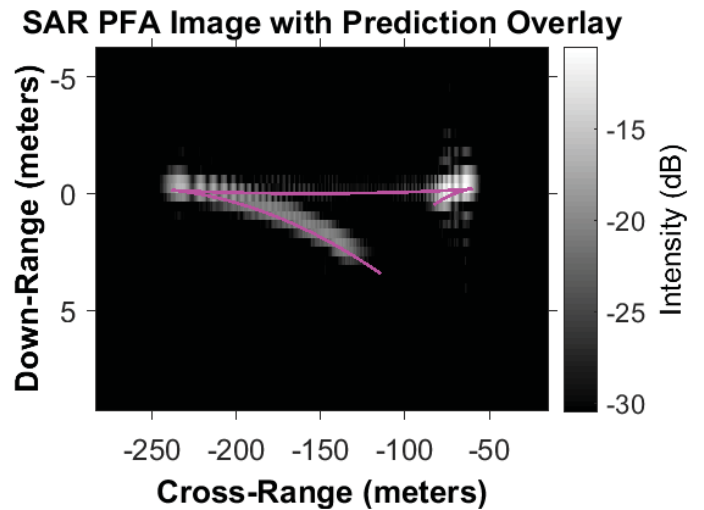
(b)

**Fig. 2:** Target trajectory and speed for the first example: (a) Target trajectory in the ground-plane, with circles at 3-second intervals; and (b) Corresponding target speed profile as a function of slow-time.

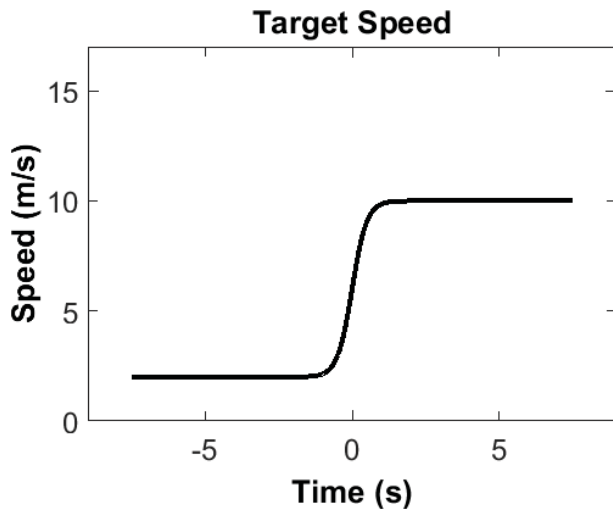
**Fig. 3:** Signature smears and prediction overlays corresponding to the target of Figure 2: (a) Rightward-pointing radar mainbeam; (b) Leftward-pointing radar mainbeam.



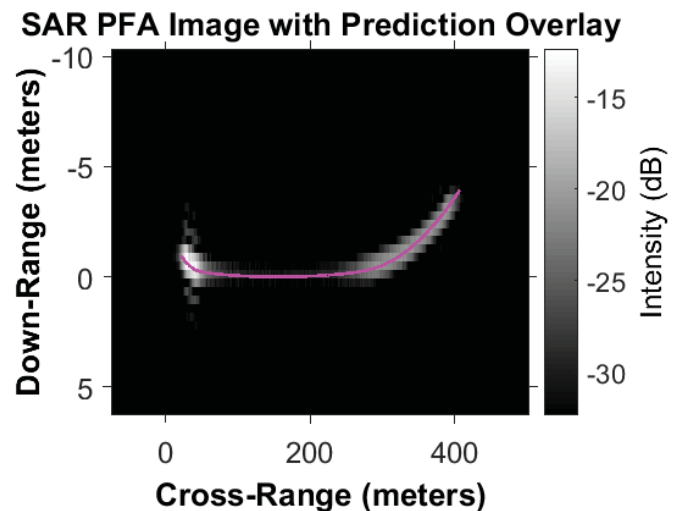
(a)



(a)



(b)



(b)

**Fig. 4:** Target trajectory and speed for the first example: (a) Target trajectory in the ground-plane, with circles at 3-second intervals; and (b) Corresponding target speed profile as a function of slow-time.

**Fig. 5:** Signature smears and prediction overlays corresponding to the target of Figure 4: (a) Rightward-pointing radar mainbeam; (b) Leftward-pointing radar mainbeam.

## 4 Conclusion

This paper examines the effects of the mean target speed on the signatures of surface movers that transition from a lower speed to a higher speed during the SAR collection interval. Such target maneuvers occur frequently in urban settings. The resulting signature shapes gave good agreement with that of the SAR simulations. A variety of signature shapes can arise, depending upon the details of the mean target speed.

## Acknowledgements

The author thanks AFRL for partial support of this work. DoD Distribution Statement A: Unlimited Distribution. The views expressed in this document are those of the author and do not reflect the official policy or position of the Department of Defense or the U.S. Government.

## References

- [1] R. K. Raney, "Synthetic aperture imaging radar and moving targets," *IEEE Transactions on Aerospace and Electronic Systems*, vol. 7, no. 3, pp. 499–505, May 1971.
- [2] R. P. Perry, R. C. DiPietro, and R. L. Fante, "SAR imaging of moving targets," *IEEE Transactions on Aerospace and Electronic Systems*, vol. 35, no. 1, pp. 188–200, Jan 1999.
- [3] J. R. Fienup, "Detecting moving targets in SAR imagery by focusing," *IEEE Transactions on Aerospace and Electronic Systems*, vol. 37, no. 3, pp. 794–809, Jul 2001.
- [4] D. Cristallini, D. Pastina, F. Colone, and P. Lombardo, "Efficient detection and imaging of moving targets in SAR images based on chirp scaling," *IEEE Transactions on Geoscience and Remote Sensing*, vol. 51, no. 4, pp. 2403–2416, Apr 2013.
- [5] J. K. Jao, "Theory of synthetic aperture radar imaging of a moving target," *IEEE Transactions on Geoscience and Remote Sensing*, vol. 39, no. 9, pp. 1984–1992, Sep 2001.
- [6] D. A. Garren, "Method and system for developing and using an image reconstruction algorithm for detecting and imaging moving targets," Patent US 7 456 780 B1, Nov 25, 2008.
- [7] X. Z. Mao and Z.-D. D.-Y. Zhu, "Signatures of moving target in polar format spotlight SAR image," *Progress in Electromagnetics Research*, vol. 92, pp. 47–64, 2009.
- [8] X. Mao, D. Zhu, L. Wang, and Z. Zhu, "Response of polar format algorithm to moving target with consideration of wavefront curvature," *2009 IEEE Radar Conference, Pasadena, CA*.
- [9] V. T. S. Vu, T. K. Pettersson, M. I. Gustavsson, A. Ulander, and M. H. Lars, "Detection of moving targets by focusing in UWB SAR - theory and experimental results," *IEEE Transactions on Geoscience and Remote Sensing*, vol. 48, no. 10, p. 3799, 2010.
- [10] R. Linnehan, L. Perlovsky, C. Mutz, and J. Schindler, "Detecting slow moving targets in SAR images," *Proceedings of SPIE 5410, Radar Sensor Technology VIII and Passive Millimeter-Wave Imaging Technology VII, 64 (August 12, 2004)*, vol. 64, Aug 2004.
- [11] X. Li, B. Deng, Y. Qin, H. Wang, and Y. Li, "The influence of target micromotion on SAR and GMTI," *IEEE Transactions on Geoscience and Remote Sensing*, vol. 49, no. 7, pp. 2738–2751, Jul 2011.

- [12] B. Deng, Y. Qin, H. Wang, and X. Li, "An efficient mathematical description of range models for high-order-motion targets in synthetic aperture radar," *Proceedings of the 2012 IEEE Radar Conference held 7-11 May 2012 in Atlanta, Georgia*, pp. 6–10, 2012.
- [13] D. A. Garren, "Smear signature morphology of surface targets with arbitrary motion in spotlight synthetic aperture radar imagery," *IET Radar, Sonar and Navigation*, vol. 8, no. 5, pp. 435–448, Jun 2014.
- [14] —, "Signatures of braking surface targets in spotlight synthetic aperture radar," *Proceedings of 2014 Sensor Signal Processing for Defence, held in Edinburgh, UK, on 08-09 September 2014*, pp. 51–55, Sep 2014.
- [15] —, "Signature predictions of surface targets undergoing turning maneuvers in spotlight synthetic aperture radar imagery," *Proceedings of SPIE, Vol. 9475, 94750A, Algorithms for Synthetic Aperture Radar Imagery XXII, 20 - 24 April 2015, in Baltimore, Maryland, USA*, pp. 4997–5008, Apr 2015.
- [16] —, "Signatures of surface targets with increasing speed in spotlight synthetic aperture radar," *2015 IEEE International Radar Conference, 11-15 May 2015 in Arlington, Virginia, USA*, p. 1114–1118, May 2015.
- [17] —, "Theory of two-dimensional signature morphology for arbitrarily moving surface targets in squinted spotlight synthetic aperture radar," *IEEE Transactions on Geoscience and Remote Sensing, Date of Publication to IEEE Xplore as an Early Access Article: 17 April 2015*, vol. 53, no. 9, pp. 4997–5008, Sep 2015.
- [18] —, "Signature morphology effects of squint angle for arbitrarily moving surface targets in spotlight synthetic aperture radar," *IEEE Transactions on Geoscience and Remote Sensing, Date of Publication to IEEE Xplore as an Early Access Article: 29 June 2015*, vol. 53, no. 11, pp. 6241–6251, Nov 2015.
- [19] R. P. Perry, R. C. DiPietro, B. L. Johnson, A. Kozma, and J. J. Vaccaro, "Planar subarray processing for SAR imaging," *IEEE International Radar Conference*, pp. 473–478, 1995.
- [20] M. Soumekh, "Digital spotlighting and coherent sub-aperture image formation for stripmap synthetic aperture radar," *Image Processing, 1994, Proceedings, ICIP-94, IEEE International Conference*, vol. 1, pp. 476–480, Nov 1994.
- [21] L. Ferro-Famil, A. Reigber, E. Pottier, and W.-M. Boerner, "Scene characterization using subaperture polarimetric SAR data," *IEEE Transactions on Geoscience and Remote Sensing*, vol. 41, no. 10, pp. 2264–2276, Oct 2003.
- [22] H. Greidanus, "Sub-aperture behavior of SAR signatures of ships," *Audio, Transactions of the IRE Profession*, pp. 794–809, 2006.
- [23] R. H. Stolt, "Migration by fourier transform," *Geophysics*, vol. 43, pp. 23–48, 1978.
- [24] S. Rahman, "Focusing moving targets using range migration algorithm in ultra wideband low frequency synthetic aperture radar," Master's thesis, Blekinge Institute of Technology, Jun 2010.